*J Appl Physiol*
90: 777–788, 2001.

# Microscopic modeling of NO and *S*-nitrosoglutathione kinetics and transport in human airways

HYE-WON SHIN[1] AND STEVEN C. GEORGE[1,2]
[1]*Department of Chemical and Biochemical Engineering and Materials Science and*
[2]*Center for Biomedical Engineering, University of California, Irvine, California 92697*

Received 28 January 2000; accepted in final form 5 September 2000

**Shin, Hye-Won, and Steven C. George.** Microscopic modeling of NO and *S*-nitrosoglutathione kinetics and transport in human airways. *J Appl Physiol* 90: 777–788, 2001.—Nitric oxide (NO) appears in the exhaled breath and is elevated in inflammatory diseases. We developed a steady-state mathematical model of the bronchial mucosa for normal small and large airways to understand NO and *S*-nitrosoglutathione (GSNO) kinetics and transport using data from the existing literature. Our model predicts that mean steady-state NO and GSNO concentrations for large airways (*generation 1*) are 2.68 nM and 113 pM, respectively, in the epithelial cells and 0.11 nM (~66 ppb) and 507 nM in the mucus. For small airways (*generation 15*), the mean concentrations of NO and GSNO, respectively, are 0.26 nM and 21 pM in the epithelial cells and 0.02 nM (~12 ppb) and 132 nM in the mucus. The concentrations in the mucus compare favorably to experimentally measured values. We conclude that *1*) the majority of free NO in the mucus, and thus exhaled NO, is due to diffusion of free NO from the epithelial cell and *2*) the heterogeneous airway contribution to exhaled NO is due to heterogeneous airway geometries, such as epithelium and mucus thickness.

exhalation; inflammation; nitric oxide

NITRIC OXIDE (NO) is a freely diffusible molecule that performs many regulatory functions, including smooth muscle relaxation, host defense, and inhibition of platelet aggregation and neurotransmission (23, 57). In addition, NO has also been detected in exhaled breath (56, 58). The fact that exhaled NO concentration increases in inflammatory airway diseases such as asthma has generated interest in using exhaled NO as a noninvasive marker of inflammation (11, 19, 24). However, the mechanisms underlying the production, consumption, and transport of NO within the lungs are not fully developed and have created difficulty in interpreting the exhaled NO signal.

Several isoforms of nitric oxide synthase (NOS) are found in many lung cell types (macrophages, vascular endothelial cells, neurons, fibroblasts, and epithelial cells) (23, 28, 43, 48, 72). Thus exhaled NO arises from both the airway and the alveolar region of the lungs and is strongly supported by theoretical studies aimed at explaining the flow rate dependence of exhaled NO (49, 65). However, even within the airways, there is evidence of heterogeneous contribution. Silkoff et al. (58) demonstrated that the main bronchus and trachea generate more than 50% of exhaled NO. Furthermore, DuBois et al. (14) evaluated equilibrium NO concentrations in the gas phase and found values that decreased from the trachea (56–266 ppb) to the respiratory bronchioles (16–41 ppb). Currently, there is no physiological explanation for this heterogeneous distribution of NO in the airway wall.

NO is a relatively reactive free radical and has a relatively short in vivo half-life (0.1–15 s) (5). *S*-nitrosoglutathione (GSNO) demonstrates NO-like bioactivity (9, 22, 31) and, due to the abundance of glutathione (GSH) in vivo, has been proposed as a possible carrier molecule for NO. GSNO degrades in the presence of GSH in a complex manner, and the major end-products are disulfide, ammonia, nitrous oxide, nitrite, and NO. When the GSH-to-GSNO ratio is high (>10), ammonia, not NO, is the most abundant end-product (61, 70). However, Gaston et al. (24) demonstrated that tracheal *S*-nitrosothiol concentration is significantly lower in asthmatic children compared with controls, whereas expired airway NO concentration is higher. From this result, Gaston et al. (24) proposed that *S*-nitrosothiol breakdown is accelerated in asthma, which leads to increased exhaled NO.

At present, there is adequate physical (dimensions and diffusivity) and chemical (rate constants and concentrations) data in the literature to begin a theoretical understanding of NO production, consumption, and transport at the cellular level in the airways to test several important hypotheses. The goal of this study is to design a plausible microscopic (cellular level) steady-state model of NO, GSH, and GSNO transport and kinetics in normal human airways. In doing so, we will address the following hypotheses: *1*) the heterogeneous airway contribution of exhaled NO is due to heterogeneity in anatomical structure and *2*) catabolism of GSNO within the mucus is a significant source of exhaled NO in normal subjects.

Address for reprint requests and other correspondence: S. C. George, Dept. of Chemical and Biochemical Engineering and Materials Science, 916 Engineering Tower, Univ. of California, Irvine, Irvine, CA 92697-2575 (E-mail: scgeorge@uci.edu).

The costs of publication of this article were defrayed in part by the payment of page charges. The article must therefore be hereby marked "*advertisement*" in accordance with 18 U.S.C. Section 1734 solely to indicate this fact.

  

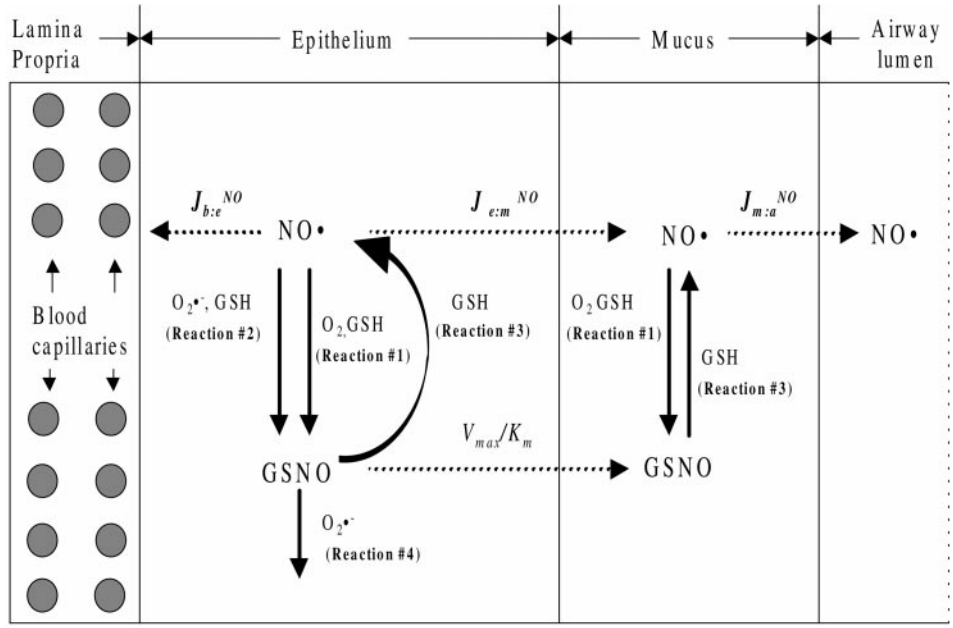


Fig. 1. Schematic of model for nitric oxide (NO) and *S*-nitrosoglutathione (GSNO) chemistry and transport in the epithelium and mucus. NO is produced in the epithelium from NO synthase (NOS) isoforms and has 3 fates: *1*) diffuses to the blood ($J_{b:e}^{NO}$), *2*) diffuses to the mucus ($J_{e:m}^{NO}$), or *3*) is consumed with oxygen or superoxide in the presence of glutathione (GSH) to produce GSNO. GSNO also has three fates: *1*) reacts with GSH to form NO (and other nitrogen products), *2*) reacts with superoxide, or *3*) is transported across the epithelial membrane. Once in the mucus, NO can diffuse into the airway lumen ($J_{m:a}^{NO}$) or react with oxygen and GSH to form GSNO, while GSNO reacts with GSH. Solid and dashed arrows represent chemical reaction and transport, respectively.

## MODEL DEVELOPMENT

*General structure.* The human conducting airways are generally considered to represent *generations 0* (trachea) to *17* (nonrespiratory bronchiole). Each airway is regarded as a cylindrical tube whose wall consists of a mucus layer, the epithelium, the lamina propria (subepithelial connective tissue), and the smooth muscle. Although the fibroblast and smooth muscle cell express NOS, they are unlikely sources of exhaled NO due to the presence of the bronchial circulation in the lamina propria and smooth muscle. NO reacts rapidly with hemoglobin, and blood is generally considered to be an infinite sink for NO (partial pressure of free NO in red blood cell $<$ 0.5 ppb). Mitochondria have been suggested as an important sink of NO due to binding to cytochrome oxidase. However, the mitochondria content in the lung is considerably lower compared with mitochondria-rich tissues such as the heart and liver. In addition, ~50% of the total mitochondria in the lung are estimated to be present within the type II alveolar cells (18). Thus we predict a small number of mitochondria in the conducting airway epithelial cells and neglect the mitochondrion sink of NO in our model.

In addition, GSNO exists as a predominantly charged molecule in vivo (acidic dissociation constant = 8.75) (1); thus, if GSNO is formed in the subepithelial tissue, free diffusion across the intercellular tight junctions (12) would be minimal. In light of the chemical and physical features of the bronchial mucosa, our model neglects the subepithelial tissue layers and considers only the epithelium and the mucous layer in understanding NO, GSH, and GSNO kinetics and transport relevant to exhaled NO.

Figure 1 depicts the model structure for the chemistry and transport of NO and GSNO in the epithelium and mucous layers. Each compartment is assumed to be "well-mixed" or of spatially uniform concentration. Conducting airway geometries for *generations 1* and *15* are listed in Table 1 and are considered to represent large and small airways, respectively. A smaller mucus layer thickness is expected in the lower generation (62). Therefore, the ratio of epithelium to mucus thickness for both *generations 1* and *15* is held constant at 10. Also, because the ratio of mucus and epithelium thickness to that of the airway diameter is $<$1, a one-dimensional Cartesian coordinate system is used.

NO is produced from NOS from the epithelial compartment, then either undergoes a chemical transformation that produces GSNO or freely diffuses to the mucus or to the bronchial circulation. GSNO is transported into the mucus via facilitated diffusion. Once in the mucus, NO and GSNO can again undergo several chemical reactions, or NO can freely diffuse into the gas phase of the airway lumen. Oxygen concentration (230 μM, equilibrium concentration with atmosphere) is identical and constant in both the epithelium and mucus due to the oxygen-rich environment in the lungs.

*Chemistry and kinetics of NO, GSH, and GSNO.* In our model, we are interested in predicting steady-state concentrations of NO and GSNO in the epithelium and mucus. To accomplish this, we must develop a chemical framework that captures the kinetic rate expressions that are likely to occur in vivo. Several reactions are documented to occur in vivo, yet most rate constants are measured in aqueous solution. Thus we assume that, within the epithelium and mucus, the reaction kinetics of NO are similar to those reported in aqueous systems.

NO can be consumed by two pathways. First, NO can react with oxygen to form the intermediate $N_2O_3$ (*reaction 1*) (29, 69). Second, NO can react with superoxide to produce peroxynitrite (*reaction 2*) (66, 71, 72). In *reaction 1*, $N_2O_3$ can react with various molecules such as water, GSH, and protein-SH. In *reaction 2*, peroxynitrite reacts predominantly with either GSH or $CO_2$. Because the intracellular and extracellular $CO_2$ concentrations are high (~1–2 mM), the peroxinitrite-$CO_2$ reaction is regarded as one of the major

Table 1. *Airway geometry*

| | *Generation 1* | *Generation 15* | Ref. |
|---|---|---|---|
| Epithelium thickness, cm | 0.010 | 0.0020 | 20 |
| Mucus thickness, cm | 0.001 | 0.0002 | 62 |

Conducting airway geometry for large (*generation 1*) and small (*generation 15*) airways.

routes for eliminating peroxinitrite. This reaction is well documented, accounting for 30–40% of the intracellular initial peroxinitrite reactivity and >90% of extracellular initial peroxinitrite reactivity. The relatively low intracellular contribution of the peroxinitrite-$CO_2$ reaction is due to a higher thiol concentration (51).

Both intermediates generate GSNO, which can subsequently be consumed by two different paths: *1*) reaction with GSH (61) (*reaction 3*) and *2*) reaction with superoxide (32) (*reaction 4*). This system of reactions is described as

$$2NO + O_2 \xrightarrow{k_{1a}} 2NO_2$$

$$NO + NO_2 \leftrightarrow N_2O_3;\ k_{1b},\ k_{-1b}$$

$$N_2O_3 + H_2O \xrightarrow{k_{1c}} 2H^+ + 2NO_2^- \qquad (\textit{Reaction 1})$$

$$N_2O_3 + GSH \xrightarrow{k_{1d}} H^+ + NO_2^- + GSNO$$

$$N_2O_3 + \text{protein} - SH \xrightarrow{k_{1e}} H^+ + NO_2^- + \text{protein} - SNO$$

$$NO + O_2^- \xrightarrow{k_{2a}} ONOO^-$$

$$ONOO^- + GSH \xrightarrow{k_{2b}} GSNO + GSSG \qquad (\textit{Reaction 2})$$

$$ONOO^- + CO_2 \xrightarrow{k_{2c}} ONOOCO_2^- \xrightarrow{k_{2d}} NO_3^- + CO_2$$

$$GSNO + GSH \xrightarrow{k_{3a}} GSSG + NH_3 + N_2O + NO_2^- + NO \qquad (\textit{Reaction 3})$$

$$2GSNO + O_2^- \xrightarrow{k_{4a}} GSSG + 2NO_2^- \qquad (\textit{Reaction 4})$$

The formulations of the kinetic rate expressions that follow from *reactions 1–4* are presented in APPENDIX A.

*Bronchial epithelium.* We assume that NO is produced from NOS at a constant rate ($\dot{S}_{NO}$), can be consumed by *reactions 1* and *2*, and can be produced or regenerated by *reaction 3*. Although the intracellular concentration of GSH (>5 mM) is high, $N_2O_3$ reacts preferentially with protein-SH, which is at even higher concentration, to generate protein-SNO. The steady state ratio of GSNO to protein-SNO is approximately 1:3 (15). Further, NO can react with superoxide to produce peroxynitrite (*reaction 2*) (34). Peroxynitrite can then react with GSH to form GSNO and disulfide (33, 34, 52, 66). Furthermore, Balazy et al. (2) demonstrated that $GSNO_2$ is produced preferentially over GSNO. Two additional studies demonstrated that GSNO formation from this reaction has a yield of <1% (27, 47). Thus we assume a mean yield of 0.2% GSNO from *reaction 2* with high uncertainty (±100%).

Generated GSNO has three fates: *1*) consumed by superoxide to give disulfide and nitrite (32), *2*) degraded by reacting with GSH, or *3*) transported to the mucous layer intact. NO is generally accepted to diffuse freely, and there is no need for a transporter system (38, 39). However, GSNO has a high potential to use a special carrier system due to a relatively large molecular weight (MW = 335.3) compared with NO and a negative charge at physiological pH. It was suggested that intracellularly generated GSNO is actively expelled from the cell, as are other *S*-substituted glutathione derivatives (60, 63). *S*-ethylglutathion (ethyl-SG), a low molecular weight and relatively hydrophilic thioether, is mainly transported across the cell membrane by an electrogenic and saturable mechanism (3). ATP increases this transport by only 10–20%. In contrast, *S*-(2,4-dinitrophenyl)-glutathione (DNP-SG), a larger and more hydrophobic anion, is transported by both ATP and voltage-dependent carriers. From these results, Ballatori and Truong (3) tentatively conclude that low molecular weight glutathione *S*-derivatives are transported largely by an electrogenic carrier system. Because GSNO is a relatively low molecular weight hydrophilic thiol, we assume GSNO to be transported by a saturable electrogenic carrier transport system characterized by Michaelis-Menten kinetics ($V_{max}$ and $K_m$) to cross the apical membrane of the epithelium (see APPENDIX B for detail).

On the basis of these assumptions and the rate expressions derived from *reactions 1–4* in APPENDIX A, the mass balances for NO and GSNO in the epithelium, a well-mixed constant volume compartment, can be written as follows for NO

$$-\frac{[\kappa_{b:e}C_{e,NO} + \kappa_{e:m}(C_{e,NO} - C_{m,NO})]}{l_e} + (k_{3a}C_{e,GSH}C_{e,GSNO} - 4k_{1a}C_{O_2}C_{e,NO}^2 - k_{2a}C_{O_2^-}C_{e,NO}) + \dot{S}_{NO} = 0 \qquad (1)$$

and for GSNO

$$-\left(\frac{V_{max}}{K_m}C_{e,GSNO}\right) - (k_{3a}C_{e,GSH}C_{e,GSNO} + k_{4a}C_{O_2^-}C_{e,GSNO}^2) + \left(\frac{k_{1d}C_{e,GSH}}{k_{1d}C_{e,GSH} + k'_{p\text{-}SH}}2k_{1a}C_{O_2}C_{e,NO}^2 + 0.002\frac{k_{2b}C_{e,GSH}}{k_{2b}C_{e,GSH} + k'_{CO_2}}k_{2a}C_{O_2^-}C_{e,NO}\right) = 0 \qquad (2)$$

where $C_{e,NO}$, $C_{m,NO}$, $C_{e,GSNO}$, $C_{e,GSH}$, and $C_{O_2^-}$ represent the molar concentrations of each species in either the epithelium (subscript e) or mucus (subscript m) and $l_e$ is the epithelium thickness. The rate constants ($k$) are defined in *reactions 1–4* or in APPENDIX A. For NO, the first term on the left-hand side represents free diffusion to either the blood or the mucus. $\kappa_{b:e}$ and $\kappa_{e:m}$ represent mass transfer coefficients between epithelium and blood and between epithelium and mucus, respectively. The mass transfer coefficients are calculated from the diffusion coefficient divided by the average length of diffusion (APPENDIX B). The second term represents consumption and production due to chemical reaction. The reaction between NO and oxygen is accelerated ~300-fold in pure hydrophobic environments such as liposomes and lipid bilayers (21, 41). However, considering that the hydrophobic membrane makes up only 4% of the volume in tissue, the actual acceleration will be a maximum of 10-fold. Although our central value for the reaction rate of NO autoxidation will be that in aqueous solution, we will consider the case in which this reaction rate is increased by ~10-fold. The third term, $\dot{S}_{NO}$, represents the production rate of NO from NOS isoforms per unit volume of tissue (55, 64).

For GSNO, the first term represents transport by an electrogenic carrier. $V_{max}/K_m$ is a transport constant defined by Michaelis-Menten kinetics (APPENDIX B). The second and third terms represent consumption and production, respectively, from chemical reaction. $k_{1d}$ and $k_{2b}$ describe GSNO formation from the reaction of NO with oxygen and/or superoxide. $k_3$ represents NO formation from GSNO decomposition due to

reaction with GSH, and $k_4$ is the GSNO consumption rate constant by superoxide. Central or mean values for all parameters are listed in Table 2.

*Mucus.* We assume that the mucous layer has the physical properties of water (i.e., diffusivity) and has a thickness of 10 μm (10) in *generation 1* and 2 μm in *generation 15*, such that the epithelium-to-mucus thickness ratio remains constant. The chemical reactions that occur in the mucus are identical to the epithelium, except the concentrations of several substrates are substantially different. Activated macrophages in the mucous layer may produce superoxide and NO as well; however, we assume that these sources are very small compared with the epithelium of normal human airways (72). GSH concentration is substantially lower (100–300 μM) than intracellular concentration and is assumed to be constant (54). Thus the reaction of the nitrosating intermediate $N_2O_3$ with GSH is competitive with hydrolysis (see APPENDIX A) (36). GSNO has a negligible vapor pressure and thus cannot enter the gas phase; however, free NO can enter the air stream by free diffusion. The gas phase resistance is negligible (10), and the mass transfer coefficient between the mucus and air is described in APPENDIX B.

On the basis of these assumptions and the rate expressions in APPENDIX A, the mass balance for NO and GSNO in the mucus can be written as

$$\text{NO: } \frac{[-\kappa_{m:a}(C_{m,NO} - C_{air}\lambda_{m:a}) + \kappa_{e:m}(C_{e,NO} - C_{m,NO})]}{l_m} + (k_{3a}C_{m,GSH}C_{m,GSNO} - 4k_{1a}C_{O_2^-}C_{m,NO}^2) = 0 \quad (3)$$

$$\text{GSNO: } \frac{V_{max}}{K_m}C_{e,GSNO} + \left(\frac{k_{1d}C_{m,GSH}}{k'_w + k_{1d}C_{m,GSH}} 2k_{1a}C_{O_2^-}C_{m,NO}^2 - k_{3a}C_{m,GSH}C_{m,GSNO}\right) = 0 \quad (4)$$

For NO, the first term on the left hand side represents free diffusion into either the gas phase or the epithelium, where $l_m$ is the mucous layer thickness and $C_{air}$ is the concentration of NO in the airway lumen. Although $C_{air}$ is strongly flow dependent (59, 65), we assume a mean constant value of 10 ppb for our steady-state simulation. The second term represents consumption and production due to chemical reaction and has been previously described.

For GSNO, the first term represents transport across the electrogenic carrier, and the second term represents consumption and production due to chemical reaction.

*Solution of governing equations. Equations 1–4* represent the steady-state mass balances for NO and GSNO in the epithelium and mucus. There are four dependent variables ($C_{e,NO}$, $C_{e,GSNO}$, $C_{m,NO}$, $C_{m,GSNO}$) and eighteen independent parameters ($k_{1a}$, $k_{1d}$, $k_{1e}$, $k_{2a}$, $k_{2b}$, $k_{3a}$, $k_{4a}$, $k'_w$, $k'_{CO_2}$, $\kappa_{b:e}$, $\kappa_{e:m}$, $\kappa_{m:a}$, $\dot{S}_{NO}$, $C_{air}$, $C_{e,GSH}$, $C_{m,GSH}$, $C_{O_2^-}$, and $V_{max}/K_m$). These four simultaneous nonlinear algebraic equations are solved by computational iteration.

*Sensitivity analysis.* The three major purposes of the sensitivity analysis are to *1*) estimate the uncertainty ranges in our predicted concentrations (model output) on the basis of uncertainties in the input parameters, *2*) identify the input parameters that have the most significant impact on the output, and *3*) establish correlation among outputs. Because our system of nonlinear algebraic equations did not have a closed form analytical solution, we chose a statistical sampling technique called Latin Hypercube Sampling (LHS) to perform the uncertainty and correlation of the output variables. McKay et al. (44, 45) evaluated three Monte Carlo types of sampling plans and demonstrated that LHS analysis is, computationally, the most efficient. LHS has been successfully used in several fields, including physiological modeling (7).

To utilize LHS, model parameter values of importance are identified and assigned central values and uncertainty ranges (Table 2). The uncertainty ranges are estimated on the basis of the accuracy of reported central values. We assigned uncertainty ranges of low (<30%), medium (50%), or high (>80%). Rate constants involving superoxide concentration ($k_{2a}$, $k_{2b}$, and $k_{4a}$) have a high uncertainty because in vivo superoxide concentration is difficult to assess. In gen-

Table 2. *Model parameters, central values, and uncertainty ranges*

| Symbol | Model Parameter | Central Value | Uncertainty | Ref. |
|---|---|---|---|---|
| $k_{1a}$ | Reaction rate constant | $2.4 \times 10^{-12}$ (nmol/l)$^{-2}$·s$^{-1}$ | ±30% | 17,35,36,40 |
| $k_{1d}$ | Reaction rate constant | $2.9 \times 10^{-4}$ (nmol/l)$^{-1}$·s$^{-1}$ | ±30% | 36 |
| $k_{2a}$ | Reaction rate constant | 4.3 (nmol/l)$^{-1}$·s$^{-1}$ | ±50% | 34 |
| $k_{2b}$ | Reaction rate constant | $1.5 \times 10^{-6}$ (nmol/l)$^{-1}$·s$^{-1}$ | ±100% | 66 |
| $k_{3a}$ | Reaction rate constant | $5.5 \times 10^{-12}$ (nmol/l)$^{-1}$·s$^{-1}$ | ±80% | 13,29 |
| $k_{4a}$ | Reaction rate constant | $9.0 \times 10^{-10}$ (nmol/l)$^{-2}$·s$^{-1}$ | ±50% | 32 |
| $k'_{p\text{-}SH}$ | Reaction rate constant | $8.7 \times 10^{-4}$ (nmol/l)$^{-1}$·s$^{-1}$ | ±100% | 15 |
| $k'_w$ | Reaction rate constant | $1.6 \times 10^{3}$ s$^{-1}$ | ±30% | 36 |
| $k'_{CO_2}$ | Reaction rate constant | $5.8 \times 10^{-5}$ (nmol/l)$^{-1}$·s$^{-1}$ | ±30% | 51 |
| $\kappa_{b:e}$ | Mass transfer coefficient from blood to epithelium | 0.0018 cm/s (*Gen. 1*)<br>0.0054 cm/s (*Gen. 15*) | ±50% | 6,16,53 |
| $\kappa_{e:m}$ | Mass transfer coefficient from epithelium to mucus | 0.0021 cm/s (*Gen. 1*)<br>0.0104 cm/s (*Gen. 15*) | ±50% | 6,16,53 |
| $\kappa_{m:a}$ | Mass transfer coefficient from mucus to airway | 0.0644 cm/s (*Gen. 1*)<br>0.3220 cm/s (*Gen. 15*) | ±50% | 6,10,16,53 |
| $\dot{S}_{NO}$ | NO production rate | 2 (nmol/l)$^{-1}$·s$^{-1}$ | ±100% | 55,64 |
| $V_{max}/K_m$ | GSNO transport constant | $1.0 \times 10^{-2}$ s$^{-1}$ | ±100% | 3 |
| $C_{e,GSH}$ | GSH concentration in epithelium | 5 mmol/l | ±80% | 36,51 |
| $C_{m,GSH}$ | GSH concentration in mucus | 200 μmol/l | ±50% | 54,67 |
| $C_{O_2^-}$ | Superoxide concentration | 0.1 nmol/l | $\log(C_{O_2^-})$ ± 100% | 50,72 |
| $C_{air}$ | Airway concentration of NO | 10.0 ppb | ±10% | 23 |

NO, nitric oxide; GSNO, *S*-nitrosoglutathione; GSH, glutathione; *Gen. 1, generation 1; Gen. 15, generation 15.* Uncertainty ranges are based on the accuracy of the reported central values.

eral, superoxide concentration is thought to range from 0.01 to 1 nM, with a mean of ~0.1 nM (34, 51). Due to this wide range, we chose a log-normal distribution such that the *log* of the superoxide concentration was equal to $-1 \pm 100\%$. High uncertainty value was also assigned to the Michaelis-Menten kinetic constant because no specific information is available for GSNO transport from epithelial cell to mucus. In contrast, $k_{1a}$, $k_{1d}$, and $C_{air}$ have relatively lower uncertainties (from $\pm 10$ to $\pm 30\%$), and the mass transfer coefficients have medium uncertainties ($\pm 50\%$) because they are relatively well characterized.

In our simulations, LHS utilized 100 model runs to achieve greater statistical significance. To accomplish this, the value for each input variable was divided into 100 equal probability density regions, based on their uncertainty. Thus, during each of the 100 model runs, a single value for each of the 18 parameters was chosen randomly and without replacement from the 100 possible values. The results of LHS were then used to generate the uncertainty in our model output by determining the mean and quartiles from the 100 runs, as well as the correlation coefficients between the outputs.

To examine the sensitivity between the 4 model output concentrations and the 18 input parameters, the relative sensitivity was estimated by a finite difference approximation (4)

$$\hat{S}(\tilde{X}, \tilde{Y}) = \left.\frac{\partial \tilde{Y}/\tilde{Y}}{\partial X_i/X}\right|_{j = 1\text{–}18, j \neq i} \approx \frac{\Delta \tilde{Y}/\tilde{Y}}{\Delta X/X} \qquad (5)$$

where $\tilde{Y}$ is the vector of the 4 model output variables, $\tilde{X}$ is the vector of the 18 input parameters, *j* refers to 18 input parameters, and *i* represents the selected input parameter. Our sensitivity is strictly local (i.e., evaluated at the central values of input parameters) and based on the change in model output concentration with a small perturbation (1%) of parameter *i* with all others held constant. Then, the sensitivity is normalized by the parameter values before perturbation for all of the parameters used to present relative sensitivity

## RESULTS

*NO and GSNO concentration in large airways.* Mean and quartiles of NO and GSNO concentrations for large airways (*generation 1*) are summarized in Table 3 and Figs. 2 and 3. It is evident from the mean and median (50% quartile) that the concentrations do not have a normal distribution. NO concentrations in the epithelium are approximately one order of magnitude larger than in mucus (Fig. 2), whereas GSNO concentrations in the epithelium are approximately three orders of magnitude smaller than in the mucus. On the basis of experimental evidence of a rapid reaction in the cell (41), increasing the reaction rate of NO autooxidation ($k_{1a}$) by 10-fold had a negligible effect on NO and slightly increased GSNO concentrations in both the epithelium and mucus (~10%). Importantly, the concentrations in the mucus compare favorably to the experimentally measured values listed in Table 4.

*NO and GSNO concentration in small airways.* For *generation 15*, our model-predicted mean and quartiles of NO and GSNO concentrations are summarized in Table 3 and Figs. 2 and 3. The patterns of NO and GSNO in the epithelium and mucus are similar to *generation 1*; however, the concentrations of both NO and GSNO are substantially smaller than in *generation 1*. Again, increasing the rate of NO autooxidation had no discernable impact on the predicted concentrations. As with *generation 1*, the mucus concentrations still compare favorably to the experimentally measured values listed in Table 4.

*Sensitivity analysis.* The estimated relative sensitivity of each parameter is summarized in Table 5, and the correlation coefficients between predicted NO and GSNO concentrations in epithelium and mucus are presented in Table 6. We are particularly interested in the parameters that impact mucus NO concentration. Values of $\hat{S} > 0.1$ are shown in Table 5. For *generation 1*, $\dot{S}_{NO}$, mass transfer, and reaction with superoxide are important parameters for both NO and GSNO. In addition to these parameters, GSNO is also sensitive to the reaction with GSH in the mucus, facilitated transport in the epithelium, and the reaction with carbon dioxide in both layers.

The relative importance of consumption by superoxide for NO is decreased from *generation 1* to *generation 15*. For *generation 15*, airway NO concentration and mass transfer from mucus to airway ($\kappa_{m:a}$) are the most important parameters for determining mucus NO concentration. Mucus NO concentration is approximately five times more sensitive to $C_{air}$ compared with that of the large airway. This reflects the relative magnitude of the mucus NO concentration in these regions (66 vs. 12 ppb) to that of $C_{air}$ (10 ppb). Also, mucus layer NO is not affected by GSNO decomposition (see *reaction 3*).

Table 3. *Mean and quartiles of NO and GSNO concentrations for generations 1 and 15*

| | $C_{e,NO}$, nM | | $C_{e,GSNO}$, pM | | $C_{m,NO}$, nM | | $C_{m,GSNO}$, nM | |
|---|---|---|---|---|---|---|---|---|
| | *Gen. 1* | *Gen. 15* | *Gen. 1* | *Gen. 15* | *Gen. 1* | *Gen. 15* | *Gen. 1* | *Gen. 15* |
| Mean | 2.68 | 0.26 | 113.34 | 21.26 | 0.11 | 0.02 | 360.16 | 75.50 |
| Quartiles | | | | | | | | |
| Minimum | 0.01 | 0.01 | 0.34 | 0.02 | 0.02 | 0.02 | 1.76 | 0.11 |
| 25% | 0.84 | 0.13 | 3.43 | 0.25 | 0.04 | 0.02 | 37.34 | 2.78 |
| 50% | 2.06 | 0.24 | 15.76 | 1.85 | 0.08 | 0.02 | 101.76 | 9.01 |
| 75% | 3.76 | 0.36 | 46.81 | 6.31 | 0.14 | 0.03 | 460.12 | 68.66 |
| Maximum | 10.59 | 0.83 | 4,323.5 | 643.0 | 0.57 | 0.04 | 5,232.9 | 2,101.5 |

$C_{e,NO}$, NO concentration in epithelium; $C_{e,GSNO}$, GSNO concentration in epithelium; $C_{m,NO}$, NO concentration in mucus; $C_{m,GSNO}$, GSNO concentration in mucus.

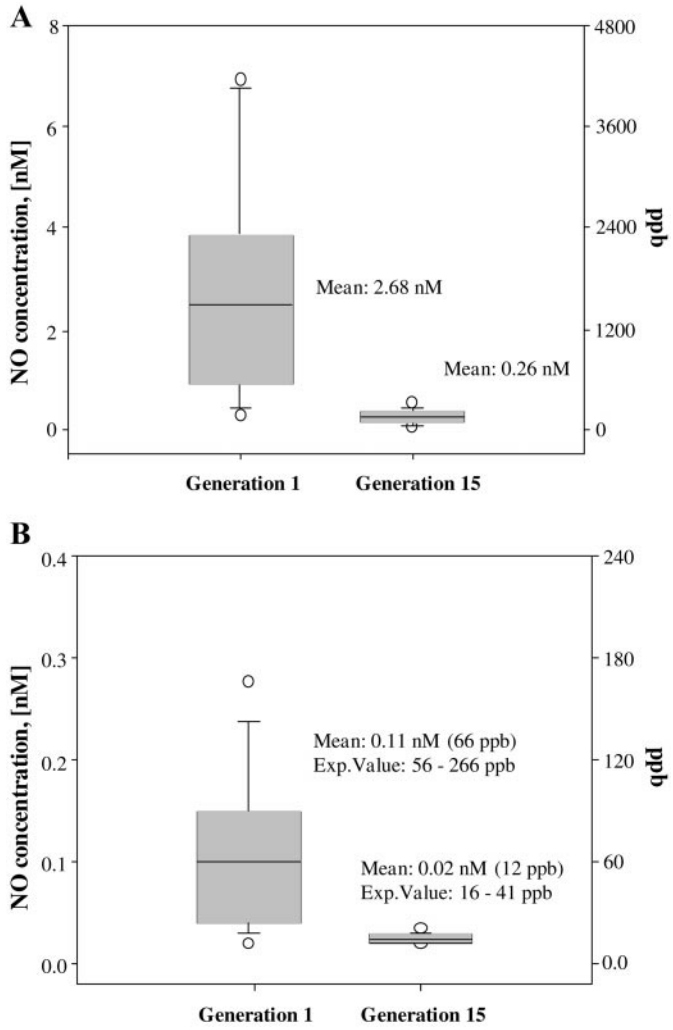


Fig. 2. NO concentrations in the epithelium (*A*) and the mucus (*B*) from the 100 model simulations of Latin Hypercube Sampling (LHS) for *generation 1* (large airways) and *generation 15* (small airways). Boxes represent 1 SD; vertical bars represent 10–90th percentiles. Lines within the boxes represent mean and median concentrations. ○, Extreme values from the 100 simulations.

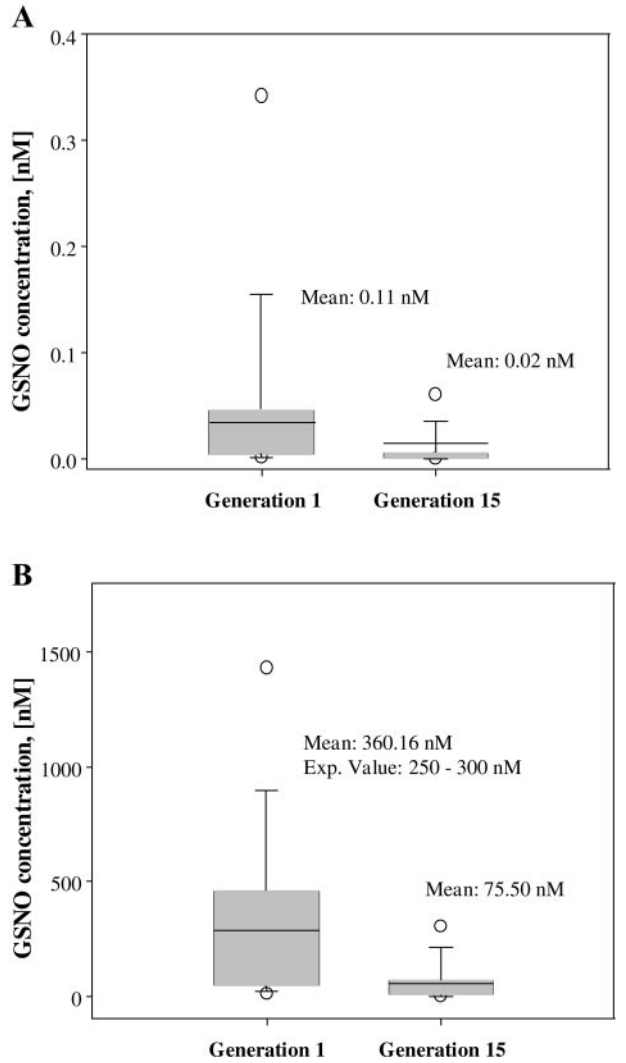


Fig. 3. GSNO concentrations in the epithelium (*A*) and the mucus (*B*) from the 100 model simulations of LHS for *generations 1* and *15*. See Fig. 2 for symbols.

Mucus NO concentration is highly correlated to epithelial NO concentration (Table 6) but not with GSNO concentration in either epithelium or mucus. This is consistent with the overall mass transfer coefficients $\kappa_{b:e}$, $\kappa_{e:m}$, and $\kappa_{m:a}$ impacting the predicted concentrations for both generations (Table 5).

## DISCUSSION

*Chemical reaction.* The epithelium is a rich environment for both superoxide and oxygen; thus NO may be consumed by either of these substrates. However, only the superoxide-mediated reaction is important within the epithelium (21), because the autooxidation of NO is very slow. This is not only evident in the sensitivity indexes (Table 5) but is also shown in Figs. 4 and 5 (NO and GSNO, respectively), which show the relative magnitude of each term in the governing equations at steady state. Note the magnitude of *reaction 1* is negligible for both NO and GSNO, but *reaction 2* is significant in the epithelium. In addition, a 10-fold acceleration in the rate of NO autoxidation (41), considering that the membrane volume in tissue is only ~4% of the total tissue volume, predicts negligible change in the predicted concentrations of NO and GSNO. This pro-

Table 4. *Experimental concentrations of NO, GSH, and GSNO in airway lining fluid*

| Species | Concentration in Airway Lining Fluid | Ref. |
|---|---|---|
| NO, ppb | | |
| Trachea | 56–266 | 14 |
| Bronchioles | 16–41 | |
| GSH, μM | 257 ± 21 | 54 |
| | 109 ± 64 | 67 |
| GSNO, μM | 0.25 | 8 |
| | 0.30 | 46 |

Table 5. *Relative sensitivity*

| | $C_{e,NO}$ | | $C_{m,NO}$ | | $C_{e,GSNO}$ | | $C_{m,GSNO}$ | |
|---|---|---|---|---|---|---|---|---|
| | *Gen. 1* | *Gen. 15* | *Gen. 1* | *Gen. 15* | *Gen. 1* | *Gen. 15* | *Gen. 1* | *Gen. 15* |
| $k_{1a}$ | | | | | | | | |
| $k_{1d}$ | | | | | | | | |
| $k_{2a}$ | −0.526 | | −0.436 | | 0.452 | 0.946 | 0.451 | 0.946 |
| $k_{2b}$ | | | | | 0.875 | 0.883 | 0.874 | 0.884 |
| $k_{3a}$ | | | | | | | −0.993 | −0.993 |
| $k_{4a}$ | | | | | | | | |
| $k'_{p\text{-}SH}$ | | | | | | | | |
| $k'_{w}$ | | | | | | | | |
| $k'_{CO_2}$ | | | | | −0.868 | −0.877 | −0.868 | −0.877 |
| $\kappa_{b:e}$ | −0.221 | −0.330 | −0.183 | −0.109 | −0.223 | −0.330 | −0.223 | −0.330 |
| $\kappa_{e:m}$ | −0.240 | −0.555 | 0.596 | 0.114 | −0.242 | −0.556 | −0.243 | −0.557 |
| $\kappa_{m:a}$ | | | −0.796 | −0.303 | | | | |
| $S_{NO}$ | 0.998 | 0.960 | 0.829 | 0.318 | 1.000 | 0.961 | 1.000 | 0.961 |
| $V_{max}/K_m$ | | | | | −0.987 | −0.987 | | |
| $C_{e,GSH}$ | | | | | 0.880 | 0.882 | 0.880 | 0.882 |
| $C_{m,GSH}$ | | | | | | | −0.990 | −0.990 |
| $C_{O_2^-}$ | −0.526 | | −0.436 | | 0.452 | 0.946 | 0.451 | 0.946 |
| $C_{air}$ | | | 0.173 | 0.682 | | | | |

Relative sensitivity was determined by using *Eq. 5* (see text for details).

vides further evidence that NO autooxidation does not impact NO concentrations in vivo.

A particularly interesting result is that GSNO catabolism (by reacting with GSH) has minimal effect on NO concentrations. This result occurs even under the extreme case of NO as the only nitrogen product. In fact, a high ratio of GSH to GSNO (>1,000) occurs in the epithelium and mucus, which would favor $NH_3$ as the end product (61, 70) and would further reduce the impact of GSNO catabolism as a source of NO. The explanation for this finding is presented in Figs. 4 and 5. It is apparent that the flux of NO due to diffusion from the epithelium is much larger than the rate of GSNO catabolism in the mucus (see *reaction 3* and Fig. 4*B*). Thus, under normal conditions, free diffusion of NO is the major source of exhaled NO, and we are forced to reject our second hypothesis.

The role of GSNO as a NO donor is under investigation, particularly in disease states such as asthma. Gaston et al. (24) suggest that GSNO catabolism is a source of NO in asthma and may proceed by a different mechanism, such as enzyme catalysis. Recent experiments by Hunt et al. (30) support this hypothesis by providing evidence for a different environment in asthma such as airway acidification. Thus the rate of reaction may be accelerated relative to the normal lungs.

Table 6. *Correlation of NO and GSNO in epithelium and mucus*

| | $C_{e,NO}$ | $C_{m,NO}$ | $C_{e,GSNO}$ | $C_{m,GSNO}$ |
|---|---|---|---|---|
| *Generation 1* | | | | |
| $C_{e,NO}$ | 1 | | | |
| $C_{m,NO}$ | 0.857 | 1 | | |
| $C_{e,GSNO}$ | 0.099 | 0.032 | 1 | |
| $C_{m,GSNO}$ | −0.074 | −0.111 | 0.175 | 1 |
| *Generation 15* | | | | |
| $C_{e,NO}$ | 1 | | | |
| $C_{m,NO}$ | 0.638 | 1 | | |
| $C_{e,GSNO}$ | 0.062 | 0.124 | 1 | |
| $C_{m,GSNO}$ | 0.093 | −0.060 | 0.224 | 1 |

Superoxide concentration is difficult to measure due to its extremely short half-life. Experimental estimates are difficult to make but suggest an intracellular concentration of ~0.01–1 nM (50, 72). In light of these characteristics of superoxide, we posed a high uncertainty (±100%) for the superoxide-mediated reactions. Under these conditions, superoxide has a large impact on GSNO concentrations in large and small airways and impacts NO in large airways. The lack of an impact of superoxide on NO in small airways is due to the smaller dimensions and, thus, an even greater role of molecular diffusion. In other words, diffusion is rapid enough that there is not sufficient time for chemical reaction with superoxide to be critical. In addition, conditions that alter superoxide levels in the lung, such as inflammatory diseases, may have a significant effect on GSNO levels. However, this source of superoxide can be from activated macrophages in the mucus, which would be an additional term in our governing equations.

*Mass transfer.* The free diffusion of NO between the bronchial circulation, the epithelium, and the airway lumen is described using three mass transfer coefficients ($\kappa_{b:e}$, $\kappa_{e:m}$, and $\kappa_{m:a}$). A linear concentration profile is not truly valid due to chemical reaction (6). In addition, there will also be mixing in the epithelium and mucus. Thus the simplifying assumptions used in APPENDIX B to estimate values for the mass transfer coefficients are only to identify central values. Thus the uncertainty posed by the LHS analysis considers the impact of mixing and chemical reaction.

As evidenced by the LHS analysis and Fig. 4, our model predicts that $\kappa_{e:m}$ and $\kappa_{m:a}$ are major parameters in determining NO in the mucus (Tables 5 and 6). In addition, if the mucus thickness is increased from 2 to

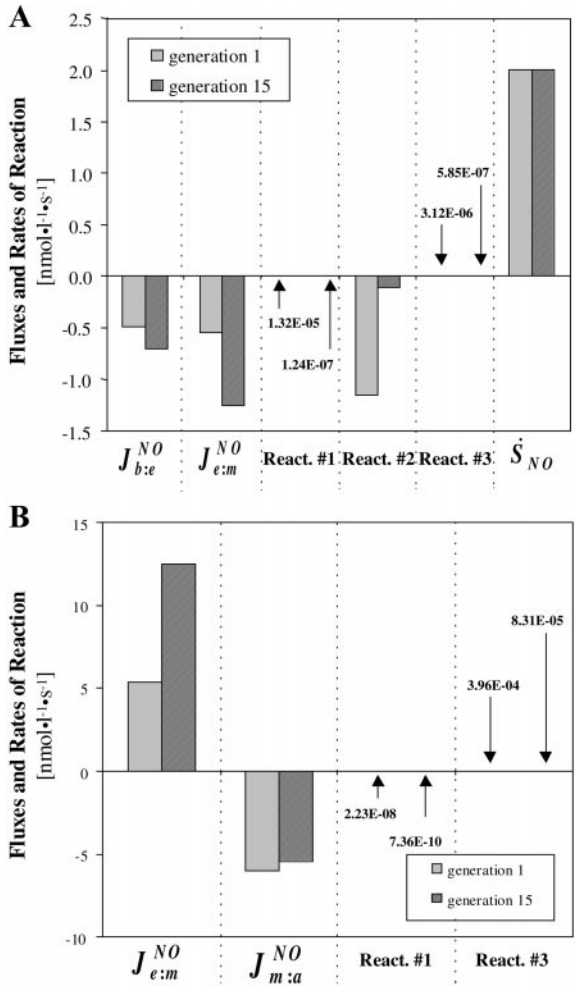


Fig. 4. Magnitude of diffusion fluxes and rates of reactions of NO at steady state for *generations 1* and *15* in the epithelium and the mucus. *A*: NO in the epithelium. *B*: NO in the mucus. Negative and positive values refer to either a decrease or increase, respectively, in NO within the compartment. Note that the ranges of values for each axis are substantially different due to the wide range of values within the compartments.

10 microns in the small airways, the flux between the mucus and airway per unit volume significantly decreases from 5.4 to 2.2 nmol·l$^{-1}$·s$^{-1}$. This decrease in the loss of NO to the air stream is due to increased resistance to diffusion through a thicker mucus layer. Thus the difference in dimensions of the epithelium and mucus in large and small airways has a profound effect on the steady-state concentrations of NO, which lends credence to our first hypothesis.

Interestingly, our model predicts that only ~25–30% of the NO produced by NOS within the epithelial cell reaches the airway lumen (Fig. 4) for *generations 1* and *15*. The bronchial circulation and superoxide (*reaction 2*) consume the remaining NO. There is substantial variability in the exhaled NO levels within normal subjects. This finding might be explained by the high sensitivity to the rate of consumption by chemical reaction with, primarily, superoxide and hemoglobin, as well as heterogeneity in the physical features of the airway mucosa. This also places critical importance on developing noninvasive indexes that characterize physical characteristics of the airways, such as tissue thickness and production rate of NO as opposed to exhaled NO concentration, if NO is to be used as a clinical indicator of inflammatory diseases.

The facilitated transport of GSNO through the cell membrane primarily impacts the epithelial concentration of GSNO. This finding reflects the relative unimportance of GSNO in determining NO concentrations that has been previously described. GSNO concentrations in the epithelial cell are predicted to be approximately three orders of magnitude smaller than in the mucus (Fig. 3), due to the fact that very little GSNO is produced (disulfide is the main oxidation product) and most of what is produced is actively transported to the

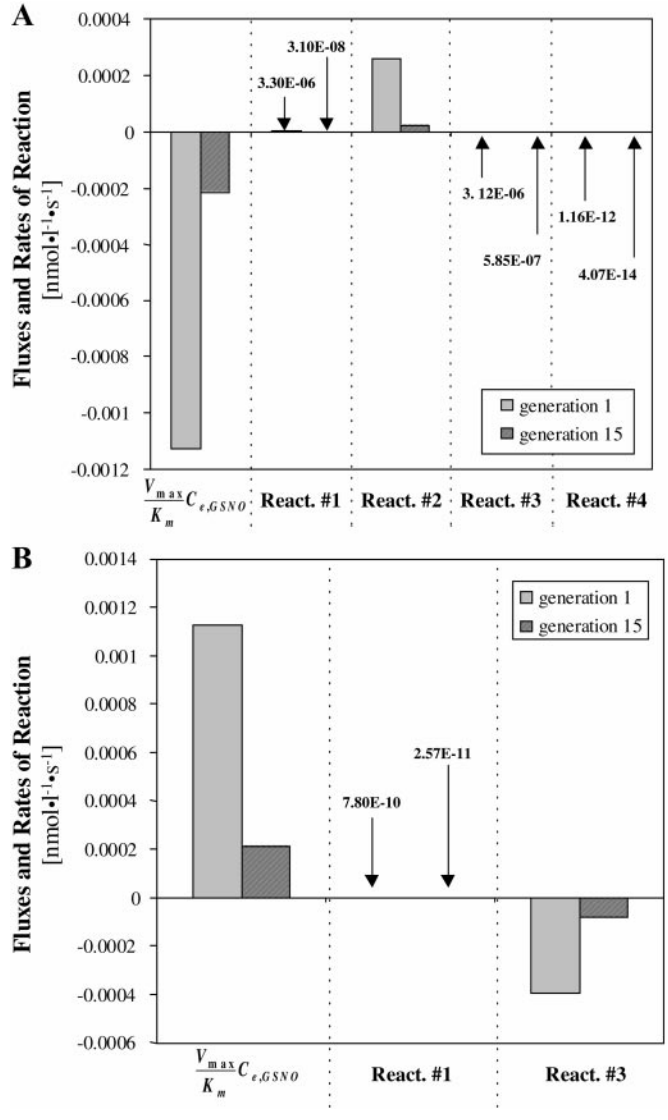


Fig. 5. Magnitude of diffusion fluxes and rates of reactions of GSNO at steady state for *generations 1* and *15* in the epithelium (*A*) and the mucus (*B*). Negative and positive values refer to either a decrease or increase, respectively, in GSNO within the compartment. Note that the ranges of values for each axis are substantially different due to the wide range of values within the compartments.

mucus. GSNO decomposition with GSH does not impact epithelial GSNO concentration, yet it is important in determining mucus GSNO concentration (Fig. 5). This finding reflects the higher GSNO concentration in the mucus layer. An electrogenic carrier for GSNO in the epithelial apical membrane does not affect mucus NO (Table 5) because changes in $V_{max}/K_m$ are offset by opposite changes in epithelial GSNO concentrations; thus the product (or net flux) remains a constant.

It is important to emphasize that no direct evidence exists for an electrogenic carrier of GSNO; however, there is strong evidence for a carrier of similar *S*-substituted glutathione derivatives (3, 60, 63). Further experimentation is necessary to document its definitive existence.

*Production rate.* The production rate of NO has a substantial impact on NO and GSNO concentrations in both the epithelial cell and the mucus. This important prediction is consistent with experimental findings in inflammatory diseases in which iNOS expression (and thus NO production rate) as well as exhaled NO is increased (i.e., increased mucus concentration of NO) (11, 72).

Previous reports reveal that the absolute amount of iNOS decreases with increasing generation number (37, 68, 72). This might suggest a decreasing production rate of NO. However, it is difficult to assess whether NO production per unit volume is changed for large and small airways. According to our simulation results, the ratio of exhaled NO concentration in *generation 1* to that of *generation 15* is ~5 (66 vs. 12 ppb). These results are consistent with the trend in the experimental data of DuBois et al. (14). According to their reported experimental data, the mean equilibrium concentration of NO in the respiratory bronchioles (16 ppb) is ~1/3 of the concentration in the larger airways (56 ppb). For our model to predict this ratio, NO production per unit volume would be ~3 times greater in the lower airways. Whereas this is certainly a possible and nonintuitive prediction, it is unlikely. A more likely explanation is that the experimental data of Dubois et al. (14) represent data from in situ airways in which a steady-state breath-to-breath NO concentration profile is established. In this scenario, upper airway NO is convected to the lower airways during inspiration, thus impacting $C_{air}$ (note the importance of $C_{air}$ in Table 5 in determining NO concentration in *generation 15*) and may impact the partial pressure of NO in the lower airways. Our simple steady-state model does not consider interaction between upper and lower airways.

In conclusion, our proposed model successfully predicts endogenous NO and GSNO concentration in the epithelium and the mucus layer for different airway generations. According to our simulation, a fraction of intracellular NO consumption leads to GSNO formation; however, the majority of free NO in the mucus layer, and thus exhaled NO, is due to diffusion of free NO from the epithelial cell and not from GSNO catabolism in normal subjects. In addition, decreasing epithelial and mucus thickness decreases steady-state NO concentrations by increasing the rate of NO lost to the blood and air by free diffusion. We conclude that free diffusion (i.e., airway geometry), chemical consumption by superoxide, and production by NOS are the critical phenomenon in understanding the dynamics of NO transport in normal human airways, and catabolism of GSNO is relatively unimportant.

## APPENDIX A

### *Rate Expressions for NO and GSNO*

*Epithelium.* REACTION 1. By applying steady-state approximation for the reaction intermediates, $NO_2$ and $N_2O_3$, one can write the following rate expressions for $C_{NO}$ and $C_{GSNO}$

$$\frac{dC_{e,NO}}{dt} = -4k_{1a}C_{e,NO}^2C_{O_2} \quad (A1)$$

$$\frac{dC_{e,GSNO}}{dt} = k_{1d}C_{e,GSH}\frac{2k_{1a}C_{e,NO}^2C_{O_2}}{k_{1c}C_{H_2O} + k_{1d}C_{e,GSH} + k_{1e}C_{p\text{-}SH}} \quad (A2)$$

where oxygen concentration is assumed to be constant at 230 μM.

Kharitonov et al. (36) demonstrated that the rate of GSNO formation is independent of GSH concentration if GSH concentration exceeds 5 mM. Also, Singh et al. (61) verified that, under excess GSH concentration, $N_2O_3$ reacts preferentially with GSH to generate GSNO. In spite of fairly high concentrations of GSH in mammalian cells (~5 mM), protein-associated thiols are present in ~3× larger quantities than low molecular weight thiols, including GSNO (15). Therefore, we consider protein-thiols as competing targets for nitrosation of $N_2O_3$ with GSH. Also, we can neglect hydrolysis of $N_2O_3$ ($k_{1c}C_{H_2O} < k_{1d}C_{GSH} + k_{1e}C_{protein\text{-}SH}$). Therefore, *Eq. A2* simplifies to

$$\frac{dC_{e,GSNO}}{dt} = \frac{2k_{1d}C_{e,GSH}}{k_{1d}C_{e,GSH} + k'_{p\text{-}SH}}k_{1a}C_{O_2}C_{e,NO}^2 \quad (A3)$$

where $k'_{p\text{-}SH} = k_{1e}C_{p\text{-}SH}$.

REACTION 2. The rate expressions for *reaction 2* can be written as follows

$$\frac{dC_{e,NO}}{dt} = -k_{2a}C_{O_2^-}C_{e,NO} \quad (A4)$$

$$\frac{dC_{e,GSNO}}{dt} = k_{2b}C_{ONOO} - C_{e,GSH} \quad (A5)$$

By applying the steady-state approximation for the intermediate peroxynitrite ($ONOO^-$), *Eq. A5* can be written as

$$\frac{dC_{e,GSNO}}{dt} = 0.002\frac{k_{2b}C_{e,GSH}}{k_{2b}C_{e,GSH} + k'_{CO_2}}k_{2a}C_{O_2^-}C_{e,NO} \quad (A6)$$

where $k'_{CO_2} = k_{2c}C_{CO_2}$. Here, we assumed that only 0.2% of the product of *reaction 2* results in GSNO formation (see text for details).

REACTION 3. Rate expressions for *reaction 3* can be written as follows, with the simplifying assumption that GSH concentration remains constant in either the epithelium or the mucus

$$\frac{dC_{e,NO}}{dt} = k_{3a}C_{e,GSH}C_{e,GSNO} \quad (A7)$$

$$\frac{dC_{e,GSNO}}{dt} = -k_{3a}C_{e,GSH}C_{e,GSNO} \quad (A8)$$

REACTION 4. The rate expression for *reaction 4* can be written as follows

$$\frac{dC_{e,GSNO}}{dt} = -k_{4a}C_{O_2^-}C_{e,GSNO}^2 \quad (A9)$$

*Mucus.* REACTION 1. The reaction mechanism is the same as reaction described for the epithelium. However, GSH concentration in the mucus (200 μM) is much lower than that in the epithelium (5 mM) (54). Therefore, the NO consumption rate is the same, but the GSNO formation reaction with $N_2O_3$ competes with its hydrolysis, and is described by

$$\frac{dC_{m,GSNO}}{dt} = \frac{2k_{1d}C_{m,GSH}}{k'_w + k_{1d}C_{m,GSH}} k_{1a}C_{O_2}C_{m,NO}^2 \quad (A10)$$

where $k'_w = k_{1c}C_{H_2O}$. In addition, we assume very low protein-associated thiols in the mucus due to relatively low membrane permeability (19).

REACTION 3. The rate mechanism is identical to that in the epithelium, with the exception that the GSH concentration is lower (200 μM).

## APPENDIX B

### *Transport Mechanisms*

*Overall mass transfer coefficients.* The flux of mass between compartments is calculated using an overall mass transfer coefficient multiplied by the mean concentration difference between the two compartments. The overall mass transfer coefficient is equivalent to a conductance or the inverse of a resistance. For simple steady-state homogeneous diffusion without chemical reaction within a slab, the mass transfer coefficient can be expressed by the diffusion coefficient of the solute in the slab divided by the length of diffusion (Fick's first law of diffusion) (6, 16). The assumption produces a linear concentration profile within the slab, which we know does not occur within a heterogeneous cell or the mucus. However, this technique can be used to identify a central value, and the uncertainty used in the LHS analysis accounts for mixing and chemical reactions.

Defining the mass transport from the midpoint of one compartment to the midpoint of an adjacent one, each overall mass transfer coefficient is then a combination of each half of adjacent layers. For example, the central value for the overall mass transfer coefficient between the epithelium and the mucus, $\kappa_{e:m}$, is described by

$$\kappa_{e:m} = \left(\frac{l_e/2}{D_e} + \frac{l_m/2}{D_m\lambda_{e:m}}\right)^{-1} \quad (A11)$$

where the first term represents the resistance from one-half of the epithelium, and second term is the resistance from one-half of the mucus. $D_e$ and $D_m$ are the diffusion coefficients of the solute (i.e., NO) in the epithelium and mucus, respectively. $\kappa_{b:e}$ and $\kappa_{m:a}$ are obtained in an analogous fashion. In addition, $\lambda_{b:e}$ and $\lambda_{e:m}$ are assumed to = 1 (26), whereas $\lambda_{m:a} = 0.0416$ for NO (64).

The diffusion coefficient of GSNO in the mucus was estimated from the Wilke-Chang method. The molar volume of solute was obtained from the additive method suggested by Schroeder (6, 53). Based on these methods, and assuming that mucus has the physical characteristics of water, the diffusion coefficient of GSNO in the mucus is $\sim 0.54 \times 10^{-5}$ cm$^2$/s. The diffusion coefficient of NO in the mucus is $\sim 3.2 \times 10^{-5}$ cm$^2$/s on the basis of an experimental measurement (42). The diffusion coefficient of NO and GSNO in the epithelium are assumed to be one-third of their value in water (25).

### *GSNO-Facilitated Transport*

We assume that GSNO is transported across the epithelial cell membrane by a transporter in the same fashion as other *S*-substituted glutathione derivatives (3). This mechanism can be expressed by Michaelis-Menten kinetics as follows

$$GSNO^e + T \overset{K_m}{\longleftrightarrow} GSNO^eT \overset{k_6}{\longrightarrow} GSNO^m + T \quad (A12)$$

where superscript e and m represent epithelial and mucus, respectively, and T represents an epithelial membrane transporter. By applying the Michaelis-Menten analysis, one can write the following rate expression for $C_{m,GSNO}$

$$\frac{dC_{m,GSNO}}{dt} = \frac{V_{max}C_{e,GSNO}}{K_m + C_{e,GSNO}} \quad (A13)$$

where $V_{max} = k_6C_T$ and $C_T$ is the concentration of transporters. *Eq. A13* then reduces to

$$\frac{dC_{m,GSNO}}{dt} = \frac{V_{max}}{K_m} C_{e,GSNO} \quad (A14)$$

for the case of $K_m > C_{e,GSNO}$ (3). As of yet, there is no exact experimental evidence for GSNO transport. Therefore, the central values of $V_{max}/K_m$ are estimated from previously reported values of *S*-substituted glutathione derivative (3).

We thank Dr. Donald Dabdub of the Dept. of Mechanical and Aerospace Engineering for helpful discussions regarding the sensitivity analysis.

This work was supported by National Science Foundation Grant BES-9875033 and National Institutes of Health Grant R29-HL-60636.

## REFERENCES

1. **Arnelle DR and Stamler JS.** $NO^+$, NO, and $NO^-$ donation by *S*-nitrosothiols: implications for regulation of physiological functions by *S*-nitrosylation and acceleration of disulfide formation. *Arch Biochem Biophys* 318: 279–285, 1995.
2. **Balazy M, Kaminski PM, Mao K, Tan J, and Wolin MS.** *S*-Nitroglutathione, a product of the reaction between peroxynitrite and glutathione that generates nitric oxide. *J Biol Chem* 273: 32009–32015, 1998.
3. **Ballatori N and Truong AT.** Multiple canalicular transport mechanisms for glutathione *S*-conjugates. Transport on both ATP- and voltage-dependent carriers. *J Biol Chem* 270: 3594–3601, 1995.
4. **Beck JV and Arnold KJ.** *Parameter Estimation in Engineering and Science.* New York: Wiley, 1977.
5. **Beckman JS and Koppenol WH.** Nitric oxide, superoxide, and peroxynitrite: the good, the bad, and ugly. *Am J Physiol Cell Physiol* 271: C1424–C1437, 1996.
6. **Bird RB, Stewart WE, and Lightfoot EN.** *Transport Phenomina.* New York: Wiley, 1960.
7. **Bui TD, Dabdub D, and George SC.** Modeling bronchial circulation with application to soluble gas exchange: description and sensitivity analysis. *J Appl Physiol* 84: 2070–2088, 1998.
8. **Butler AR and Rhodes P.** Chemistry, analysis, and biological roles of *S*-nitrosothiols. *Anal Biochem* 249: 1–9, 1997.
9. **Clancy RM, Levartovsky D, Leszczynska-Piziak J, Yegudin J, and Abramson SB.** Nitric oxide reacts with intracellular glutathione and activates the hexose monophosphate shunt in human neutrophils: evidence for i-nitrosoglutathione as a bioactive intermediary. *Proc Natl Acad Sci USA* 91: 3680–3684, 1994.

10. **Condorelli P and George SC.** Theoretical gas phase mass transfer coefficients for endogenous gases in the lungs. *Ann Biomed Eng* 27: 326–339, 1999.
11. **Crater SE, Peters EJ, Martin ML, Murphy AW, and Platts-Mills TA.** Expired nitric oxide and airway obstruction in asthma patients with an acute exacerbation. *Am J Respir Crit Care Med* 159: 806–811, 1999.
12. **Crystal RG and West JB.** *The Lung: Scientific Foundations.* New York: Raven, 1991, p. 157–167, 197–203, 205–214, 263–271.
13. **Dicks AP, Li E, Munro AP, Swift HR, and Williams DLH.** The reaction of *S*-nitrosothiols with thiols at high thiol concentration. *Can J Chem* 76: 789–794, 1998.
14. **DuBois AB, Kelley PM, Douglas JS, and Mohsenin V.** Nitric oxide production and absorption in trachea, bronchi, bronchioles, and respiratory bronchioles of humans. *J Appl Physiol* 86: 159–167, 1999.
15. **Eu JP, Liu L, Zeng M, and Stamler JS.** An apoptotic model for nitrosative stress. *Biochem J* 39: 1040–1047, 2000.
16. **Fogler HS.** *Elements of Chemical Reaction Engineering.* Englewood Cliffs, NJ: Prentice-Hall, 1992.
17. **Ford PC, Wink DA, and Stanbury DM.** Autoxidation kinetics of aqueous nitric oxide. *FEBS Lett* 326: 1–3, 1993.
18. **Forfia PR, Hintze TH, Wolin MS, and Kaley G.** Role of nitric oxide in the control of mitochondrial function. *Adv Exp Med Biol* 471: 381–388, 1999.
19. **Frank TL, Adisesh A, Pickering AC, Morrison JF, Wright T, Francis H, Fletcher A, Frank PI, and Hannaford P.** Relationship between exhaled nitric oxide and childhood asthma. *Am J Respir Crit Care Med* 158: 1032–1036, 1998.
20. **Gastineau RM, Walsh PJ, and Underwood N.** Thickness of bronchial epithelium with relation to exposure to radon. *Health Phys* 23: 857–860, 1972.
21. **Gaston B.** Nitric oxide and thiol groups. *Biochim Biophys Acta* 1411: 323–333, 1999.
22. **Gaston B, Drazen JM, Jansen A, Sugarbaker DA, Loscalzo J, Richards W, and Stamler JS.** Relaxation of human bronchial smooth muscle by *S*-nitrosothiols in vitro. *J Pharmacol Exp Ther* 268: 978–984, 1994.
23. **Gaston B, Drazen JM, Loscalzo J, and Stamler JS.** The biology of nitrogen oxides in the airways. *Am J Respir Crit Care Med* 149: 538–551, 1994.
24. **Gaston B, Sears S, Woods J, Hunt J, Ponaman M, McMahon T, and Stamler JS.** Bronchodilator *S*-nitrosothiol deficiency in asthmatic respiratory failure. *Lancet* 351: 1317–1319, 1998.
25. **George SC, Babb AL, and Hlastala MP.** Dynamics of soluble gas exchange in the airways. III. Single-exhalation breathing maneuver. *J Appl Physiol* 75: 2439–2449, 1993.
26. **George SC, Babb AL, and Hlastala MP.** Modeling the concentration of ethanol in the exhaled breath following pretest breathing maneuvers. *Ann Biomed Eng* 23: 48–60, 1995.
27. **Graves JE, Lewis SJ, and Kooy NW.** Peroxynitrite-mediated vasorelaxation: evidence against the formation of circulating *S*-nitrosothiols. *Am J Physiol Heart Circ Physiol* 274: H1001–H1008, 1998.
28. **Head CA.** Nitric oxide and the lung: an overview. *Artif Organs* 21: 5–9, 1997.
29. **Hogg N, Singh RJ, and Kalyanaraman B.** The role of glutathione in the transport and catabolism of nitric oxide. *FEBS Lett* 382: 223–228, 1996.
30. **Hunt JF, Fang K, Malik R, Snyder A, Malhotra N, Platts-Mills TA, and Gaston B.** Endogenous airway acidification. Implications for asthma pathophysiology. *Am J Respir Crit Care Med* 161: 694–699, 2000.
31. **Jansen A, Drazen J, Osborne JA, Brown R, Loscalzo J, and Stamler JS.** The relaxant properties in guinea pig airways of *S*-nitrosothiols. *J Pharmacol Exp Ther* 261: 154–160, 1992.
32. **Jourd'heuil D, Mai CT, Laroux FS, Wink DA, and Grisham MB.** The reaction of S-nitrosoglutathione with superoxide. *Biochem Biophys Res Commun* 246: 525–530, 1998.
33. **Karoui H, Hansert B, Sand PJ, Tordo P, Bohle DS, and Kalyanaraman B.** Spin-trapping of free radicals formed during the oxidation of glutathione by tetramethylammonium peroxynitrite. *Nitric Oxide* 1: 346–358, 1997.
34. **Karoui H, Hogg N, Fréjaville C, Tordo P, and Kalyanaraman B.** Characterization of sulfur-centered radical intermediates formed during the oxidation of thiols and sulfite by peroxynitrite. ESR-spin trapping and oxygen uptake studies. *J Biol Chem* 271: 6000–6009, 1996.
35. **Keshive M, Singh S, Wishnok JS, Tannenbaum SR, and Deen WM.** Kinetics of *S*-nitrosation of thiols in nitric oxide solutions. *Chem Res Toxicol* 9: 988–993, 1996.
36. **Kharitonov VG, Sundquist AR, and Sharma VS.** Kinetics of nitrosation of thiols by nitric oxide in the presence of oxygen. *J Biol Chem* 270: 28158–28164, 1995.
37. **Kobzic L, Bredt DS, Lowenstein CJ, Drazen J, Gaston B, Sugarbaker D, and Stamler JS.** Nitric oxide synthase in human and rat lung: immunocytochemical and histochemical localization. *Am J Respir Cell Mol Biol* 9: 371–377, 1993.
38. **Lancaster JR Jr.** Simulation of the diffusion and reaction of endogenously produced nitric oxide. *Proc Natl Acad Sci USA* 91: 8137–8141, 1994.
39. **Lancaster JR Jr.** A tutorial on the diffusibility and reactivity of free nitric oxide. *Nitric Oxide* 1: 18–30, 1997.
40. **Lewis RS and Deen WM.** Kinetics of the reaction of nitric oxide with oxygen in aqueous solutions. *Chem Res Toxicol* 7: 568–574, 1994.
41. **Liu X, Miller MJS, Joshi MS, Thomas DD, and Lancaster JR Jr.** Accelerated reaction of nitric oxide with $O_2$ within the hydrophobic interior of biological membranes. *Proc Natl Acad Sci USA* 95: 2175–2179, 1998.
42. **Malinski T, Taha Z, Grunfeld S, Patton S, Kapturczak M, and Tomboulian P.** Diffusion of nitric oxide in the aorta wall monitored in situ by porphyrinic microsensors. *Biochem Biophys Res Commun* 193: 1076–1082, 1993.
43. **Marletta MA.** Nitric oxide synthase: aspects concerning structure and catalysis. *Cell* 78: 927–930, 1994.
44. **McKay MD, Beckman RJ, and Conover WJ.** A comparison of three methods for selecting values of input variables in the analysis of output from a computer code. *Technometrics* 21: 239–245, 1979.
45. **McKay MD, Conover WJ, and Whiteman DE.** Report on the application of statistical techniques to the analysis of computer codes (Informal report). Los Alamos, CA: Los Alamos Scientific Laboratory of the University of California, 1976.
46. **Meyer DJ, Kramer H, Ozer N, Coles B, and Ketterer B.** Kinetics and equilibria of S-nitrosothiol-thiol exchange between glutathione, cysteine, penicillamines, and serum albumin. *FEBS Lett* 345: 177–180, 1994.
47. **Moro MA, Darley-Usmar VM, Goodwin DA, Read NG, Zamora-Pino R, Feelisch M, Radomski MW, and Moncada S.** Paradoxical fate and biological action of peroxynitrite on human platelets. *Proc Natl Acad Sci USA* 91: 6702–6706, 1994.
48. **Nathan C and Xie QW.** Nitric oxide synthases: roles, tolls, and controls. *Cell* 78: 915–918, 1994.
49. **Pietropaoli AP, Perillo IB, Torres A, Perkins PT, Frasier LM, Utell MJ, Frampton MW, and Hyde RW.** Simultaneous measurement of nitric oxide production by conducting and alveolar airways of humans. *J Appl Physiol* 87: 1532–1542, 1999.
50. **Pryor WA.** *Natural Antioxidants in Human Health and Disease.* San Diego, CA: Academic, 1994.
51. **Radi R.** Peroxynitrite reactions and diffusion in biology. *Chem Res Toxicol* 11: 720–721, 1998.
52. **Radi R, Beckman JS, Bush KM, and Freeman BA.** Peroxynitrite oxidation of sulfhydryls. The cytotoxic potential of superoxide and nitric oxide. *J Biol Chem* 266: 4244–4250, 1991.
53. **Reid RC, Prausnitz JM, and Poling BE.** *The Properties of Gases and Liquids* (4th ed.). New York: McGraw-Hill, 1987.
54. **Roum JH, Buhl R, McElvaney NG, Borok Z, and Crystal RG.** Systemic deficiency of glutathione in cystic fibrosis. *J Appl Physiol* 75: 2419–2424, 1993.
55. **Samouilov A, Kuppusamy P, and Zweier JL.** Evaluation of the magnitude and rate of nitric oxide production from nitrite in biological systems. *Arch Biochem Biophys* 357: 1–7, 1998.
56. **Schedin U, Frostell C, Persson MG, Jakobsson J, Andersson G, and Gustafsson LE.** Contribution from upper and lower

airways to exhaled endogenous nitric oxide in humans. *Acta Anaesthesiol Scand* 39: 327–332, 1995.
57. **Schmidt HH and Walter U.** NO at work. *Cell* 78: 919–925, 1994.
58. **Silkoff PE, McClean PA, Caramori M, Slutsky AS, and Zamel N.** A significant proportion of exhaled nitric oxide arises in large airways in normal subjects. *Respir Physiol* 113: 33–38, 1998.
59. **Silkoff PE, McClean PA, Slutsky AS, Furlott HG, Hoffstein E, Wakita S, Chapman KR, Szalai JP, and Zamel N.** Marked flow-dependence of exhaled nitric oxide using a new technique to exclude nasal nitric oxide. *Am J Respir Crit Care Med* 155: 260–267, 1997.
60. **Singh RJ, Hogg N, Joseph J, and Kalyanaraman B.** Mechanism of nitric oxide release from *S*-nitrosothiols. *J Biol Chem* 271: 18596–18603, 1996.
61. **Singh SP, Wishnok JS, Keshive M, Deen WM, and Tannenbaum SR.** The chemistry of the *S*-nitrosoglutathione/glutathione system. *Proc Natl Acad Sci USA* 93: 14428–14433, 1996.
62. **Sleigh MA, Blake JR, and Liron N.** The propulsion of mucus by cilia. *Am Rev Respir Dis* 137: 726–741, 1988.
63. **Stamler JS.** *S*-nitrosothiols and the bioregulatory actions of nitrogen oxides through reactions with thiol groups. *Curr Top Microbiol Immunol* 196: 19–36, 1995.
64. **Tsoukias NM and George SC.** A two-compartment model of pulmonary nitric oxide exchange dynamics. *J Appl Physiol* 85: 653–666, 1998.
65. **Tsoukias NM, Tannous Z, Wilson AF, and George SC.** Single-exhalation profiles of NO and $CO_2$ in humans: effect of dynamically changing flow rate. *J Appl Physiol* 85: 642–652, 1998.
66. **Vliet AVD, Hoen PACT, Wong PSY, Bast A, and Cross CE.** Formation of *S*-nitrosothiols via direct nucleophilic nitrosation of thiols by peroxynitrite with elimination of hydrogen peroxide. *J Biol Chem* 273: 30255–30262, 1998.
67. **Vliet AVD, O'Neill CA, Cross CE, Koostra JM, Volz WG, Halliwell B, and Louie S.** Determination of low-molecular-mass antioxidant concentrations in human respiratory tract lining fluids. *Am J Physiol Lung Cell Mol Physiol* 276: L289–L296, 1999.
68. **Watkins DN, Peroni DJ, Basclain KA, Garlepp MJ, and Thompson PJ.** Expression and activity of nitric oxide synthases in human airway epithelium. *Am J Respir Cell Mol Biol* 16: 629–639, 1997.
69. **Wink DA, Nims RW, Darbyshire JF, Christodoulou D, Hanbauer I, Cox GW, Laval F, Laval J, Cook JA, Krishna MC, Degraff WG, and Mitchell JB.** Reaction kinetics for nitrosation of cysteine and glutathione in aerobic nitric oxide solutions at neutral pH. Insights into the fate and physiological effects of intermediates generated in the $NO/O_2$ reaction. *Chem Res Toxicol* 7: 519–525, 1994.
70. **Wong PS, Hyun J, Fukuto JM, Shirota FN, DeMaster EG, Shoeman DW, and Nagasawa HT.** Reaction between *S*-nitrosothiols and thiols: generation of nitroxyl (HNO) and subsequent chemistry. *Biochem J* 37: 5362–5371, 1998.
71. **Wu M, Pritchard KA Jr, Kaminski PM, Fayngersh RP, Hintze TH, and Wolin MS.** Involvement of nitric oxide and nitrosothiols in relaxation of pulmonary arteries to peroxynitrite. *Am J Physiol Heart Circ Physiol* 266: H2108–H2113, 1994.
72. **Zapol WM and Bloch KD.** *Nitric Oxide and the Lung.* New York: Dekker, 1997. (Lung Biol. Health Dis. Ser., vol. 98).